UC Irvine
UC Irvine Previously Published Works

Title

Selective cooling of biological tissues: application for thermally mediated therapeutic procedures

Permalink

https://escholarship.org/uc/item/7b26r9cs

Journal

Physics in Medicine and Biology, 40(2)

ISSN

0031-9155

Authors

Anvari, B
Milner, TE
Tanenbaum, BS
et al.

Publication Date

1995-02-01

DOI

10.1088/0031-9155/40/2/003

Copyright Information

This work is made available under the terms of a Creative Commons Attribution License, availalbe at
https://creativecommons.org/licenses/by/4.0/

Peer reviewed

Selective cooling of biological tissues: application for thermally mediated therapeutic procedures

Bahman Anvari†, Thomas E Milner†, B Samuel Tanenbaum‡, Sol Kimel§,
Lars O Svaasand‖ and J Stuart Nelson†

† Beckman Laser Institute and Medical Clinic, University of California, Irvine, CA, USA
‡ Department of Engineering, Harvey Mudd College, Claremont, CA, USA
§ Department of Chemistry, Technion-Israel Institute of Technology, Haifa, Israel
‖ Division of Physical Electronics, University of Trondheim, Norwegian Institute of
Technology, Trondheim, Norway

Abstract. The ability to control the degree and spatial distribution of cooling in biological tissues during a thermally mediated therapeutic procedure would be useful for several biomedical applications of lasers. We present a theory based on the solution of the heat conduction equation that demonstrates the feasibility of selectively cooling biological tissues. Model predictions are compared with infrared thermal measurements of *in vivo* human skin in response to cooling by a cryogen spurt. The presence of a boundary layer, undergoing a liquid–vapour phase transition, is associated with a relatively large thermal convection coefficient (≈ 40 kW m^{-2} K^{-1}), which gives rise to the observed surface temperature reductions (30–40 °C). The degree and the spatial-temporal distribution of cooling are shown to be directly related to the cryogen spurt duration.

1. Introduction

Selective cooling of biological tissues whereby the degree and spatial distribution of cooling can be achieved in a controlled manner would be of benefit for several therapeutic procedures in dermatology where the objective of treatment is to produce irreversible thermal damage to subsurface tissue constituents without destroying or altering superficial structures. Examples of such procedures include laser treatment of port wine stains (PWS), telangiectasias, and a haemangiomas in which the ideal therapeutic outcome is photothermolysis of subsurface dermal blood vessels without damage to the normal overlying epidermis (Anderson and Parris 1983). Selective cooling would also be beneficial in the clinical management of patients with other dermatoses, such as dermal melanocytic lesions and tattoos (Nelson 1991).

We present a theory, which incorporates thermal and radiometric considerations, that demonstrates the feasibility of selectively cooling biological tissues. Experiments that use infrared radiometry to measure the thermal response of *in vivo* human skin to cooling by a cryogen spurt are conducted to verify the theoretical results. The heat transfer process resulting from cryogen cooling and the potential dermatologic application to laser treatment of PWS are discussed.

2. Theory

2.1. Heat transfer

We assume a two-layered semi-infinite medium consisting of skin in contact with a cold film whose thickness may change with time (figure 1). Since the film is in contact with both air and skin, we refer to it as a 'boundary layer' (bl) and interpret its formation as follows. During the time course of a cryogen spurt, skin temperature is reduced as a result of supplying the latent heat of vaporization. As the skin surface temperature approaches the boiling point of the cryogen, the rate at which cryogen droplets evaporate becomes less than the accumulation rate. Consequently, a boundary layer of thickness $d(t)$, consisting of a mixture of cryogen and ice (resulting from condensation), is formed on the skin surface at a constant growth rate of $\dot{d}$ (micrometres per second).
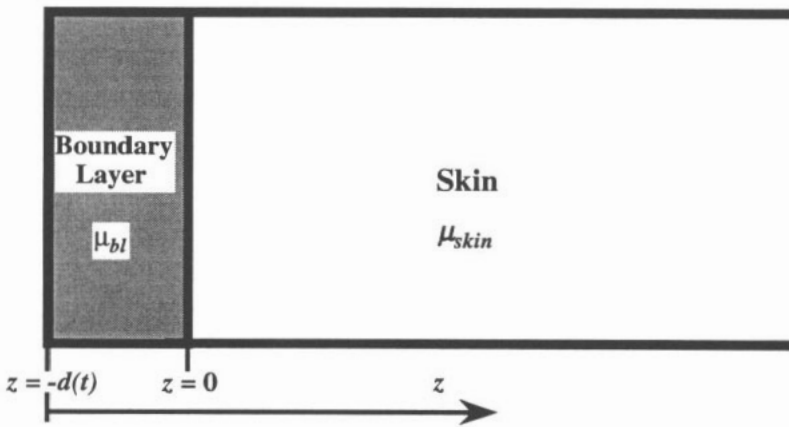

Figure 1. A two-layered geometry consisting of skin in contact at $z = 0$ with a cold and infrared attenuating boundary layer of varying thickness $d(t)$.

Assuming uniform thermal properties and neglecting blood perfusion and sources of internal heat generation (e.g. tissue metabolism), temperature distributions within skin, $T(z > 0, t)$, for the case where the lateral dimensions of the cooled area are much larger than the thermal penetration depth, are calculated by solving the one-dimensional heat conduction equation,

$$\partial^2 T(z, t)/\partial z^2 = (1/\alpha)\partial T(z, t)/\partial t \tag{1}$$

where $T(z, t)$ (degrees Celsius) is the temperature at time t (seconds) and position z (metres), and α is the thermal diffusivity of skin (1.1×10^{-7} m^2 s^{-1}) (Duck 1990). When cooling the skin by formation of a cold boundary layer, a convective boundary condition is imposed at the skin–film interface:

$$k[\partial T(z, t)/\partial z]|_{z=0} = h[T_\infty - T(0, t)] \tag{2}$$

where k (watts per metre per kelvin) is the thermal conductivity of skin (0.45 W m^{-1} K^{-1}) (Duck 1990), h (watts per square metre per kelvin) is the thermal convection coefficient (a

quantity not known *a priori*) and T_∞ (degrees Celsius) is the temperature of the boundary layer (i.e. $T(-d < z < 0) = T_\infty$ is assumed to be constant). Using the method of Laplace transformation, the solution to equation (1) with the given boundary condition (equation (2)) and a uniform initial temperature, $T(z > 0, t = 0) = T_0$ is (Carslaw and Jaeger 1959)

$$T(z > 0, t) = (T_\infty - T_0)\{\operatorname{erfc}(\tilde{z}) - [\exp(\tilde{h}^2 + 2\tilde{h}\tilde{z})\operatorname{erfc}(\tilde{h} + \tilde{z})]\} + T_0 \qquad (3)$$

where

$$\tilde{z} = z/2\sqrt{\alpha t} \qquad \tilde{h} = (h/k)\sqrt{\alpha t} \qquad (4)$$

and $\operatorname{erfc}(x)$ is the complementary error function, $1 - \operatorname{erfc}(x)$.

According to equation (3) and assuming $T_\infty = -10\,^\circ\mathrm{C}$, a large surface temperature drop ($\approx 40\,^\circ\mathrm{C}$) is obtained within a short time (of the order of milliseconds) (figure 2) when h is relatively large (e.g. $h = 40$ kW m^{-2} K^{-1}), consistent with the presence of a boundary layer undergoing a liquid–vapour phase transition (Incropera and Dewitt 1981). For relatively small values of h (e.g. $h = 0.4$ kW m^{-2} K^{-1}), associated with free convection or forced convection by a gas, only a small temperature drop ($\sim 2\,^\circ\mathrm{C}$) is obtained.
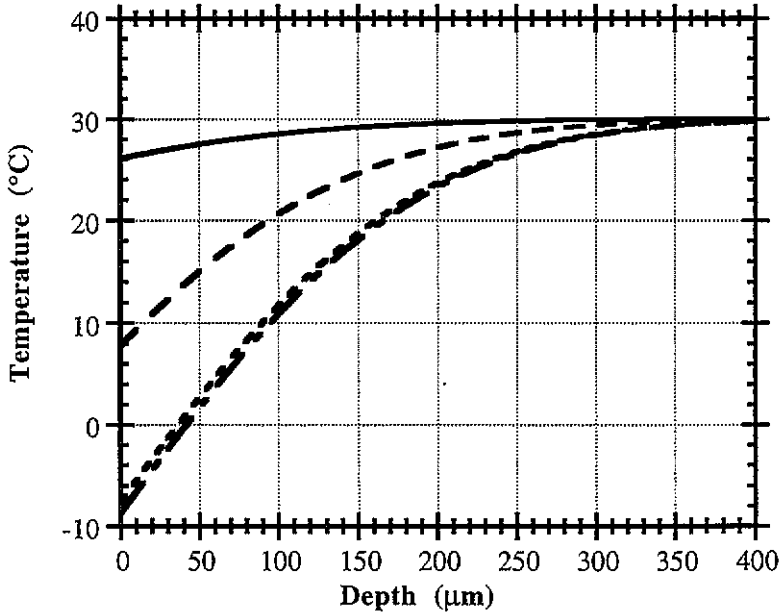

Figure 2. Spatial temperature distributions, $T(z, t = 100$ ms$)$, after a cryogen spurt duration $\tau = 100$ ms, with T_∞ fixed at $-10\,^\circ\mathrm{C}$, for the indicated values of the convection coefficient, h (kW m^{-2} K^{-1}): ——, 0.4; – – –, 4; - - - -, 40; — · —, 90.

The instantaneous heat flux, q (watts per square metre), at the skin surface is

$$q(t) = -k[\partial T(z, t)/\partial z]|_{z=0} = h[T_\infty - T(0, t)] = h(T_\infty - T_0)\exp(\tilde{h}^2)\operatorname{erfc}(\tilde{h}) \qquad (5)$$

and the energy removed per unit area, Q (joules per square metre), is

$$Q(t) = \int_0^t q(t')\,\mathrm{d}t = \frac{k^2(T_\infty - T_0)}{h\alpha}\left\{\frac{2\tilde{h}}{\sqrt{\pi}} + [\exp(\tilde{h}^2)\operatorname{erfc}(\tilde{h})] - 1\right\}. \qquad (6)$$

2.2. Radiometrics

Let $E_{b,\Delta\lambda}(T(z,t))$ (watts per square metre) be the emissive power of a black body within a spectral bandwidth, $\Delta\lambda$, at a prescribed temperature. Expanding $E_{b,\Delta\lambda}(T(z,t))$ in a Taylor series about the initial temperature, T_0, and keeping the first two terms in the series gives

$$E_{b,\Delta\lambda}(T(z,t)) \approx E_{b,\Delta\lambda}(T_0) + [\partial E_{b,\Delta\lambda}(T(z,t))/\partial T(z,t)]|_{T=T_0}[T(z,t) - T_0]. \tag{7}$$

The measured radiometric signal, $\Delta S(t)$ (degrees Celsius), is proportional to the change in the emissive power of a black body at a prescribed temperature within the spectral bandwidth $\Delta\lambda$ (i.e. proportional to $E_{b,\Delta\lambda}(T(z,t)) - E_{b,\Delta\lambda}(T_0)$, and is computed by integrating the attenuated infrared emission over all depths. For the two-layered semi-infinite medium shown in figure 1,

$$\Delta S(t) = C \int_{-d(t)}^{\infty} [T(z,t) - T_0]\mu_{ir}(z) \exp\left(-\int_{-d(t)}^{z} \mu_{ir}(z')\,dz'\right) dz \tag{8}$$

where $\mu_{ir}(z)$ (per metre) is the infrared attenuation coefficient, assumed to be constant over the spectral bandwidth $\Delta\lambda$, and C is a calibration factor that is related to the product of the term $[\partial E_{b,\Delta\lambda}(T(z,t))/\partial T(z,t)]|_{T=T_0}$ and the specific infrared detection system characteristics (e.g. detector area and responsivity).

With $\mu_{ir}(z) = \mu_{bl}$ for $-d(t) < z < 0$, and $\mu_{ir}(z) = \mu_{skin}$ for $z > 0$, the integral in the argument of the exponential function in equation (8) is evaluated as

$$\int_{-d(t)}^{z} \mu_{ir}(z')\,dz' = \begin{cases} \mu_{bl}[z + d(t)] & \text{for } -d(t) < z < 0 \\ \mu_{bl}d(t) + \mu_{skin}z & \text{for } z > 0. \end{cases} \tag{9}$$

Substituting equation (9) into equation (8),

$$\Delta S(t) = C\mu_{bl} \int_{-d(t)}^{0} [T(z,t) - T_0] \exp\{[-\mu_{bl}(z + d(t))]\}\,dz$$

$$+ C\mu_{skin} \int_{0}^{\infty} [T(z,t) - T_0] \exp[-\mu_{bl}d(t) - \mu_{skin}z]\,dz. \tag{10}$$

Using the expressions for $T(z,t)$ given in subsection 2.1, equation (10) becomes

$$\Delta S(t) = C(T_\infty - T_0)\{1 - \exp[-\mu_{bl}d(t)]\} + C(T_\infty - T_0)$$

$$\times \exp[-\mu_{bl}d(t)]\{1 - \{(h/k)\exp[(\mu_{skin}\sqrt{\alpha t})^2]$$

$$\times \text{erfc}(\mu_{skin}\sqrt{\alpha t}) - \mu_{skin}\exp(\tilde{h}^2)\text{erfc}(\tilde{h})\}/[(h/k) - \mu_{skin}]\}. \tag{11}$$

$\Delta S(t)$ denotes the 'radiometric temperature' change in the presence of an attenuating boundary layer. The two terms on the RHS of equation (11) represent, from left to right, the attenuated infrared emission from the boundary layer and skin, respectively.
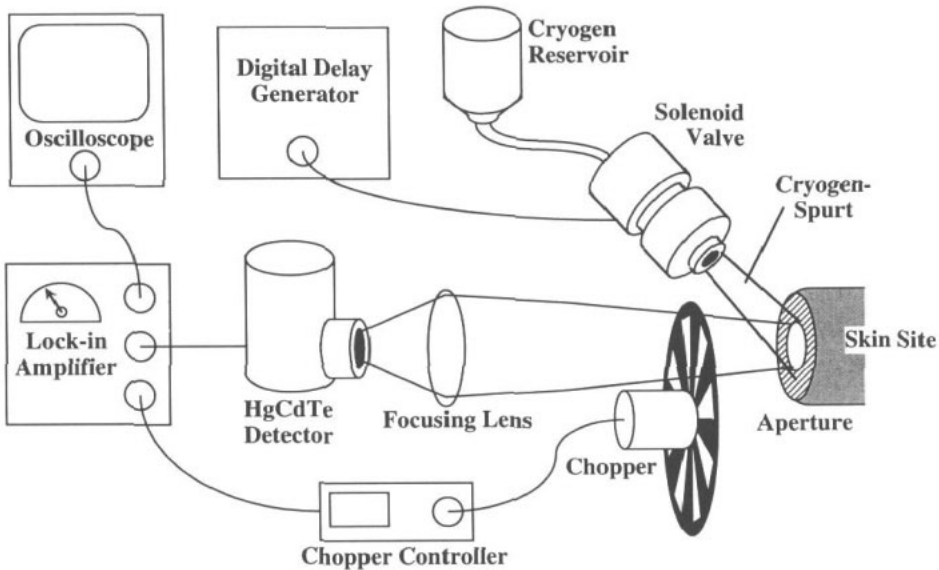
Figure 3. The experimental set-up for cooling the skin and measuring the radiometric temperature.

3. Methods and materials

In vivo human skin on fingers and forearm was cooled with a cryogen spray (1,1,1,2-tetrafluoroethane, $C_2H_2F_4$, an environmentally compatible, non-toxic, non-flammable freon substitute, BP $= -26.2\,°C$) (figure 3). Cryogen was contained in a pressurized steel canister ($\sim$ 5 atm), and delivered through an electronically controlled standard fuel injection valve (aperture diameter $\approx$ 1 mm) covering a 7 mm diameter area on the skin. The duration of the cryogen spurt, τ (5–80 ms), was controlled by a programmable digital delay generator (DG535, Stanford Research Systems). The distance between the aperture of the solenoid valve and the skin surface was maintained at 20 mm.

Infrared emission from the cooled skin site was detected using a 1 mm^2 liquid N_2 cooled HgCdTe detector (MDD-10E0-S1, Cincinnati Electronics) placed at the focal plane of a 25 mm diameter f/1 Ge lens, and optically filtered by a 7–11 μm bandpass filter (RL-7500-F, Corion). The collection optics was configured for unit magnification and had an exit pupil of 5 mm diameter positioned 50 mm from the detector, resulting in an f/10 system. The optical axis was oriented normal to the cooled skin site. For improved signal to noise ratio, the infrared radiation was amplitude modulated (3 kHz) using a mechanical chopper, and synchronously detected by a lock-in amplifier (SR850, Stanford Research Systems).

The temperature response of the detection system was calibrated by measuring the lock-in amplifier voltage as a function of the surface temperature of an Al block, coated with highly emissive ($\varepsilon \approx 0.97$) black paint (TC-303 black, GIE Corp.), and heated from 23 to 45 °C by a resistive element. The surface temperature of the Al block was measured using a precision thermistor (8681, Keithley) attached to the block; the measured voltage was proportional to the surface temperature (1.05 mV °C^{-1}).

In order to investigate the effect of stratum corneum thickness on the measured infrared signal, we compared spraying skin on fingers to that on the forearm where the stratum

corneum is thinner. The skin water content is known to increase from the surface towards the stratum corneum–granulosum interface (Bommannan *et al* 1990, von Zglinick *et al* 1993). Thus, the radiometric temperature in response to a cryogen spurt at these anatomical sites may be different under similar experimental conditions. Each site was sprayed eight times for a given τ and the resulting signals averaged.

A Michelson interferometer using an He–Ne laser ($\lambda = 632$ nm) as a coherent light source was used to estimate the thickness of the boundary layer. One mirror of the interferometer was sprayed with the cryogen and the resulting boundary layer thickness, d, was related to the number of fringes, N, and the index of refraction of the cryogen, n (assumed to be ≈ 1.5), as

$$d = N\lambda/2(n - 1). \tag{12}$$

4. Results

The radiometric temperature showed a rapid decrease (figure 4) in response to spraying the skin for various spurt durations. For $\tau = 5$ ms, an immediate radiometric temperature reduction to $0\,°C$ was measured; longer spurts resulted in radiometric temperatures between $-4\,°C$ and $-10\,°C$. After termination of the cryogen spurt the radiometric temperature began to increase. Increased spurt duration resulted in a longer relaxation time to the initial baseline temperature.
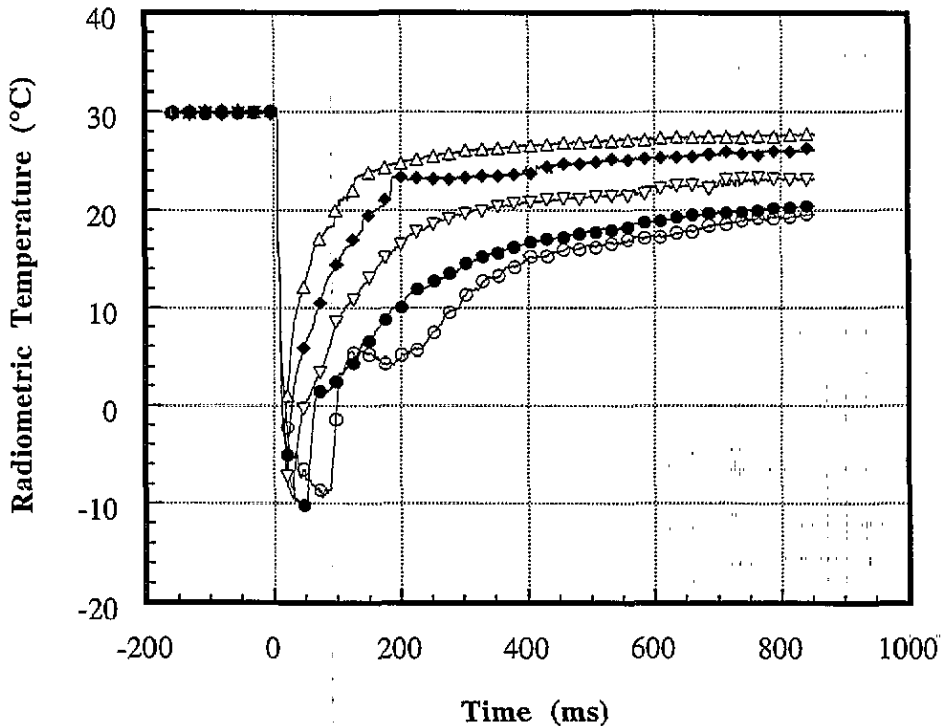

Figure 4. The *in vivo* radiometric temperature of skin (fingers) in response to cryogen spurts of duration 5 ms (—△—△—), 10 ms (—◆—◆—), 20 ms (—▽—▽—), 40 ms (—●—●—) and 80 ms (—○—○—).

For $\tau = 80$ ms, ice formation (presumably by condensation of water vapour present in the air) on the skin surface was observed. Measurements using laser interferometry indicated the thickness of the boundary layer to be ~ 20 μm. The presence of a quasiequilibrium state, during which the temperature was constant for ~ 100 ms, is probably due to ice–liquid (i.e. melting) and/or ice–vapour (i.e. sublimation) phase transitions. For shorter spurt durations, smaller quantities of ice may have formed, resulting in an imperceptible phase transition time.

Measurements of the thermal response of fingers and forearm for $\tau = 5$ ms are shown in figure 5: spraying the forearm consistently resulted in significantly lower radiometric temperatures. A discussion of this observation is presented later (section 5).
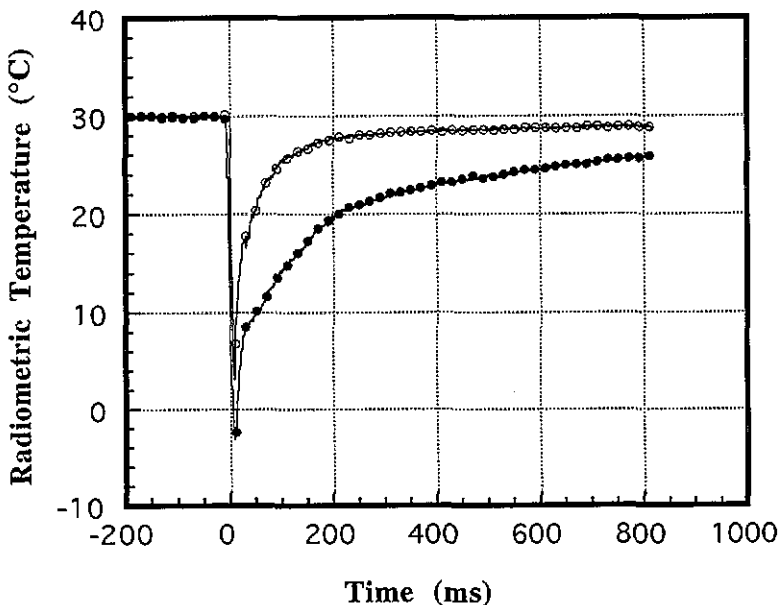

Figure 5. The *in vivo* radiometric temperature of skin in response to a spurt duration of 5 ms: fingers, —O—O—; forearm, —●—●—.

Infrared emission is attenuated as it propagates through the boundary layer. The infrared spectrum of H_2O ice in the 7–11 μm spectral region is characterized by an absorption coefficient $\mu_{ir} \sim 0.1$–0.3 μm^{-1} (Bertie and Whalley 1964, Johari 1981, Hudgins *et al* 1993). Gaseous tetrafluoroethane shows four absorption peaks in this region (McFarland 1994). To our knowledge, there is no reported value for the infrared attenuation coefficient of liquid tetrafluoroethane. Therefore, we performed a parametric study of the effect of μ_{bl} on the radiometric temperature (figure 6). Values of h and T_∞ were set to 40 kW m^{-2} K^{-1} and $-10\,^\circ$C, respectively. Considering that water is the major constituent of the skin, we used $\mu_{skin} = 0.06$ μm^{-1}, characteristic of liquid water in the 7–11 μm spectral region (Hale and Querry 1973, Marechal 1991).

For a 20 μm thick film that accumulates in 80 ms ($\dot{d} = 0.25$ μm ms^{-1}), increased infrared attenuation by the boundary layer is predicted to result in lower values of the radiometric temperature. As infrared attenuation of the boundary layer increases, there is a greater contribution to the detected signal from the boundary layer and the radiometric temperature approaches that of the boundary layer. Conversely, as $\mu_{bl} \to 0$, the detected signal originates from the skin.
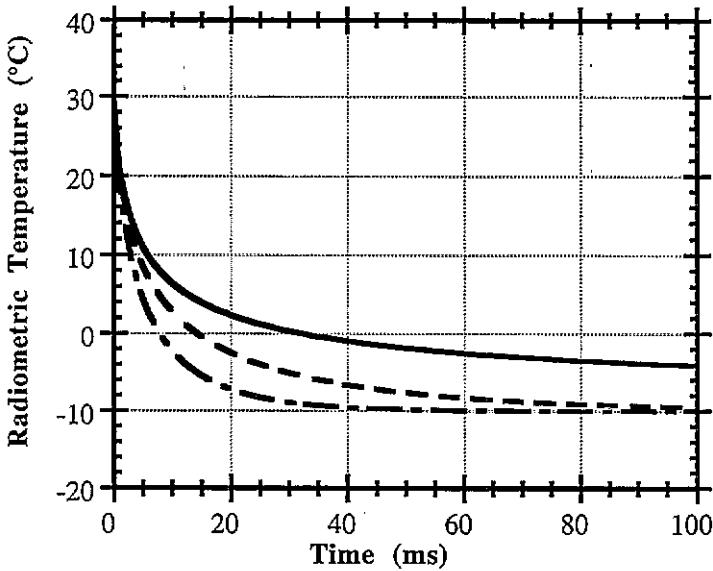
Figure 6. The effect of varying the infrared attenuation μ_{ir} of the boundary layer on the computed radiometric temperature: ——, 0; – – –, 0.1 μm^{-1}; — · —, 0.3 μm^{-1}; for $h = 40$ kW m^{-2} K^{-1} and $T_\infty = -10\,°C$.

The physical model of the boundary layer described above gives good agreement with infrared thermal measurements for all spurt durations; we present results for $\tau = 80$ ms (figure 7). We used $h = 40$ kW m^{-2} K^{-1} and $T_\infty \approx -9\,°C$ to fit the results of the radiometric temperature for the fingers (figure 7(a)), and $h = 90$ kW m^{-2} K^{-1} and $T_\infty \approx -11\,°C$ to fit the results of the measurements on the forearm (figure 7(b)). Values of $\mu_{bl} = 0.3$ μm^{-1} and $\dot{d} = 0.25$ μm ms^{-1} were used in both cases. Values of h are well within the range of known heat transfer coefficients representing convective heat transfer due to a liquid–vapour phase transition (Incropera and Dewitt 1981).

To examine the uniqueness of the parameters used in fitting the experimental data, a sensitivity study on T_∞ and $\dot{d}$ revealed that T_∞ had a more pronounced effect on the predicted temperatures. As T_∞ was lowered by a factor of two, the radiometric surface temperature decreased by a few degrees ($\sim 3\,°C$) in the first few milliseconds and approached T_∞ with increasing time. Increasing $\dot{d}$ by a factor of two resulted in a reduction of the radiometric surface temperature by about $2\,°C$ in the first few milliseconds without affecting the response for $t > 30$ ms.

The instantaneous heat flux, q, at the skin surface is maximum at the instant when the cryogen is deposited, as the induced thermal gradient is greatest at this time (figure 8). After 10 ms, the heat flux has diminished appreciably, whereas the total amount of heat removed at the surface, Q, continues to increase, albeit both at reduced rates.

Calculated values of $T(z)$ within skin (using $h = 40$ kW m^{-2} K^{-1}, and $T_\infty \approx -9\,°C$) illustrate the feasibility of selectively cooling biological tissue (figure 9). The duration of the cryogen spurt can be used to control the degree and spatial/temporal distribution of cooling in tissue. For example, locations 20 μm below the surface can be cooled by $20\,°C$ in response to a cryogen spurt of $\tau = 20$ ms duration, while temperatures of deeper layers located below 100 μm remain unchanged. At positions below 300 μm, temperatures are unaffected by the spurt duration (for $\tau \leqslant 80$ ms).
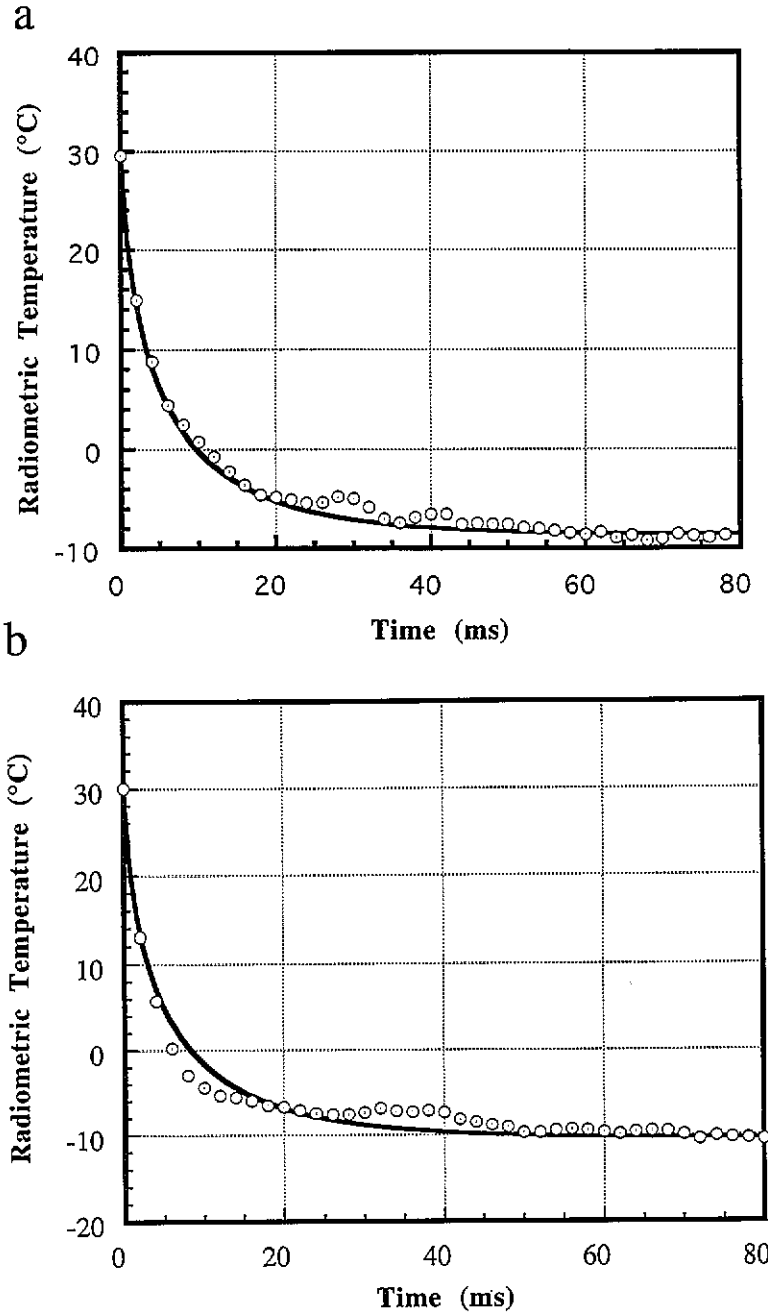
a

b

Figure 7. A comparison of the computed (——) and measured (O) radiometric temperature, for a cryogen spurt duration $\tau = 80$ ms, of (a) fingers and (b) forearm.

5. Discussion

Our theory predicts that temperature reductions to less than 0 °C at the skin surface can be obtained by large thermal convection coefficients that are associated with a liquid–vapour
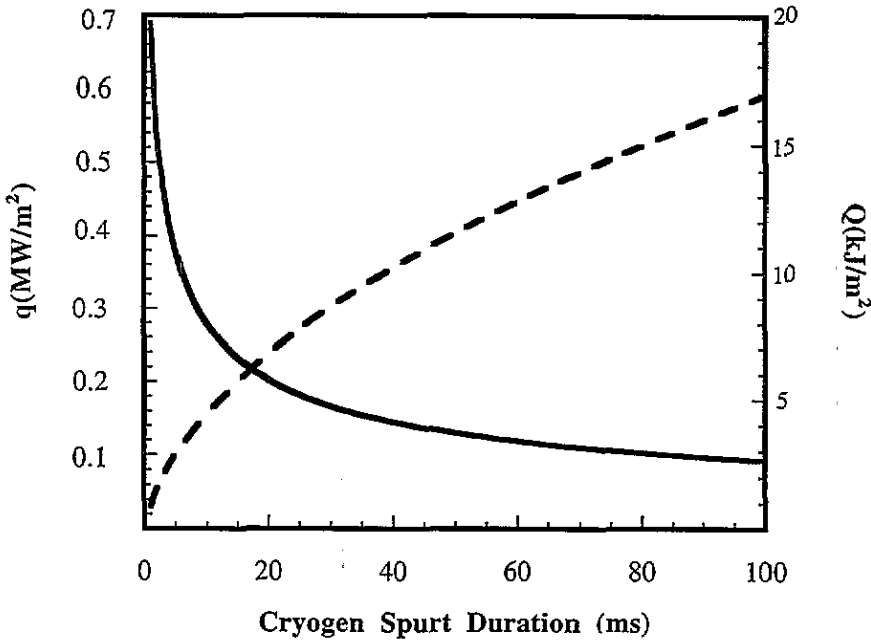
Figure 8. Computed values of the instantaneous heat flux, *q* (megawatts per square metre) (——), and the total energy, *Q* (kilojoules per square metre) (– – –) as a function of cryogen spurt duration (τ), for $h = 40$ kW m^{-2} K^{-1} and $T_{\infty} \approx -9\,°$C.

phase transition (figure 2). Spraying the skin with millisecond duration cryogen spurts provides an effective method for inducing such temperature reductions. Liquid cryogen droplets (BP $= -26.5\,°$C) strike the 'hot' (30 °C) skin surface and undergo evaporation. Skin temperature is reduced as a result of supplying the latent heat of vaporization. As the skin surface temperature approaches the boiling point of the cryogen, the thermal energy supplied by the skin is no longer sufficient to vaporize the impinging cryogen droplets. At this stage, the droplets begin to accumulate on the skin surface, creating a boundary layer consisting of cryogen droplets and ice (due to condensation of water vapour present in the surrounding air). The exact temperature of the boundary layer, somewhere between the cryogen boiling temperature and 0 °C, is determined by the relative amounts of cryogen and ice.

At the end of a cryogen spurt, the thermal gradient established within the skin causes diffusion of heat from the warmer deeper layers toward the cold surface. The supplied heat results in increased surface temperatures, evaporation of cryogen droplets, and melting/sublimation of ice. For an 80 ms spurt, evaporation of cryogen and ice ·is completed in about 100 ms (figure 4).

When spraying the fingers and forearm, lower radiometric temperatures were measured on the latter (figure 5). This observation may be explained by the increased hydration of the stratum corneum from the surface towards the stratum corneum–spinosum (deeper layer of the epidermis) interface (Bommannan *et al* 1990, von Zglinick *et al* 1993). On the forearm, where the stratum corneum is thinner, infrared emission from layers below the stratum corneum is attenuated due to increased water content. In this case a greater portion
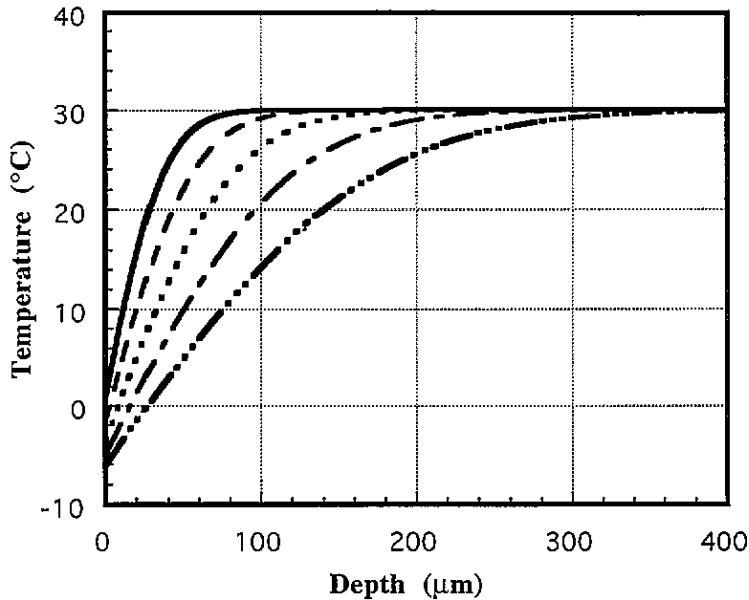
Figure 9. The computed temperature distribution, $T(z, t = \tau)$, within the skin for different spurt durations τ, for $h = 40$ kW m^{-2} K^{-1} and $T_\infty = -9\,°$C: ———, 5 ms; – – –, 10 ms; - - - -, 20 ms; — · —, 40 ms; —· · ·—· · ·, 80 ms.

of the detected infrared signal originates from the more superficial, less attenuating layers of skin. Conversely, on the fingers, where the stratum corneum is thicker, a greater portion of the detected infrared signal originates from the deeper and warmer layers. Therefore, on the fingers, the infrared detection system probes deeper into the skin and the radiometric temperature in response to a cryogen spurt is expected to be higher than for corresponding measurements on the forearm (figure 7). An equivalent explanation can be presented in terms of emissivity rather than absorbance of water.

Selective cooling of tissue as an integral part of a therapeutic procedure could be useful for various biomedical applications, for example in the laser treatment of PWS. Ideally, such a treatment method should result in irreversible thermal damage to blood vessels that comprise the PWS while preserving the normal overlying epidermis. Encouraging results have been reported in a preliminary clinical study using millisecond cryogen spurts to protect the skin surface from damaging thermal effects associated with light absorption by epidermal melanin (Nelson *et al* 1994). However, further development of the cooling strategy is needed for optimal treatment of PWS. For example, the relative timing between laser irradiation and cryogen spurt delivery is important. When irradiating with a flashlamp pumped pulsed dye laser, an effective strategy might be one that delivers a laser pulse during a relatively long spurt. Prior to laser irradiation, cooling reduces the temperature in the pigmented epidermis, while the presence of the boundary layer during and after laser exposure provides a heat sink for dissipation of epidermal heat generated by melanin absorption. Studies are currently under way in our laboratory to examine the resulting thermal response of skin to cryogen spray cooling during laser irradiation.

6. Conclusions

We have developed a theory for radiometric temperature in the presence of an attenuating convective boundary layer in contact with a semi-infinite medium. The theory, in combination with radiometric temperature measurements, can be used to estimate the value of the convective heat transfer coefficient.

The time controlled formation of a boundary layer on the skin surface can be used for selective cooling. The liquid–vapour phase transition of a cryogen (e.g. tetrafluoroethane) is sustained by heat transferred from the skin and results in subsequent cooling of tissue. Large temperature drops (30–$40\,^\circ$C) in thin superficial layers (50–$150\ \mu$m) are obtained in short periods of time (5–80 ms). The degree and spatial/temporal distribution of tissue cooling can be achieved in a controlled manner by adjusting the cryogen spurt duration.

References

Anderson R R and Parrish J A 1983 Selective photothermolysis: precise microsurgery by selective absorption of pulsed radiation *Science* **220** 524–7
Bertie J E and Whalley E 1964 Infrared spectra of ices I_L and I_C in the range 4000 to 350 cm^{-1} *J. Chem. Phys.* **40** 1637–45
Bommannan D, Potts R O and Guy R 1990 Examination of stratum corneum barrier function in vivo by infrared spectroscopy *J. Invest. Dermatol.* **95** 403–8
Carslaw H S and Jaeger J C 1959 *Conduction of Heat in Solids* 2nd edn (Oxford: Clarendon)
Duck F A 1990 *Physical Properties of Tissue. A Comprehensive Reference Book* (London: Academic)
Hale G M and Querry M R 1973 Optical constants of water in the 200 nm to 200 μm wavelength region *Appl. Opt.* **12** 555–63
Hudgins D M, Sandford S A, Allamandola L J and Tielens G G M 1993 Mid- and far-infrared spectroscopy of ices: optical constants and integrated absorbance *Astrophys J. Suppl. Ser.* **86** 713–870
Incropera F P and Dewitt D P 1981 *Fundamentals of Heat and Mass Transfer* 2nd edn (New York: Wiley)
Johari G P 1981 The spectrum of ice *Contemp. Phys.* **22** 613–42
Marechal Y 1991 Infrared spectra of water. I. Effect of temperature and H/D isotopic dilution *J. Chem. Phys.* **95** 5565–73
McFarland M 1994 Personal communication
Nelson J S 1991 Selective photothermolysis and removal of cutaneous vasculopathies and tattoos by pulsed laser *Plastic Reconstruc. Surg.* **88** 723–31
Nelson J S, Milner T E, Anvari B, Tanenbaum B S, Kimel S, Svaasand L O and Jacques S L 1994 Dynamic epidermal cooling during pulsed laser treatment of port wine stain—a new methodology with preliminary clinical evaluation *Arch. Dermatol.* at press
von Zglinick T, Lindberg M, Roomans G M and Forsland B 1993 Water and ion distribution profiles in human skin *Acta Derm. Venereol.* **73** 340–3